Multimode Interference Couplers With Reduced Parasitic Reflections

Emil Kleijn, Daniele Melati, Andrea Melloni, Tjibbe de Vries, Meint K. Smit, and Xaveer J. M. Leijtens

***Abstract*— Parasitic reflections can deteriorate the performance of a photonic integrated circuit. This is especially true in circuits containing amplifiers, but even in passive circuits, small reflections can already have a strong influence on circuit performance. It is known that strong reflections can be present when using a 2 × 1 multimode interference coupler (MMI) as a combiner. We investigate methods for reducing these spurious reflections in a generic integration technology. We present a novel MMI shape whose measurements show reduced reflections by 17.5 dB.**

***Index Terms*— Integrated optics, optical waveguides, optical couplers.**

I. Introduction

MULTIMODE interference couplers (MMIs) are frequently used as splitters and combiners in photonic integrated circuits (PICs). However, because they contain abrupt junctions, these components are liable to generate parasitic reflections [1]. These reflections can disturb the desired behavior of the circuit. In circuits containing amplifiers, parasitic reflections may cause gain ripples or even unwanted lasing. In this letter we discus a new geometry to suppress parasitic reflections in MMI couplers. We will focus on 1 × 2 MMIs, as they are known to be especially liable to generate reflections when used as combiners [2].

When used as a splitter, 1×2 MMIs divide light efficiently over the two output waveguides. Due to limited imaging resolution, some light will be imaged on the back edge of the MMI. The index step present there causes some light to scatter back to the input. In splitter operation the amount of back-scattered light is very low because almost all the light ends up in the output waveguides. This is not the case when using the same MMI as a combiner. Only when light in the two inputs is coherent, in phase, and of equal magnitude, will it be efficiently coupled to the output waveguide. When only the fundamental mode in one input is present, no more than half of the light will be coupled to the fundamental mode of the output waveguide for reciprocity reasons. The other half of the light will be scattered and some of it reflected backwards. This reflection process can be highly efficient due to the imaging properties of the MMI [2]–[4].

Manuscript received September 16, 2013; revised November 29, 2013; accepted December 16, 2013. Date of publication December 20, 2013; date of current version January 24, 2014. This work was supported by the European Community's Seventh Framework Programme FP7/2007-2013 under Grant Agreement ICT 257210 PARADIGM.

E. Kleijn, T. de Vries, M. K. Smit, and X. J. M. Leijtens are with the COBRA Research Institute, Eindhoven University of Technology, Eindhoven 5600 MB, The Netherlands (e-mail: e.kleijn@tue.nl; t.d.vries@tue.nl; m.k.smit@tue.nl; x.j.m.leijtens@tue.nl).

D. Melati and A. Melloni are with the Dipartimento di Elettronica, Informazione e Bioingegneria, Politecnico di Milano, Milano 20133, Italy (e-mail: melati@elet.polimi.it; melloni@elet.polimi.it).

Color versions of one or more of the figures in this letter are available online.

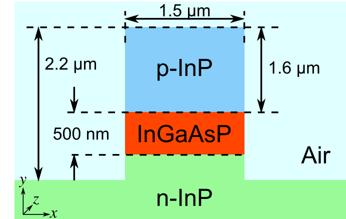

Fig. 1. The COBRA layer stack. The layer thicknesses and composition are indicated.

Previous attempts to reduce the reflection level of 2×1 MMI combiners used lossy waveguides [2], or reduced contrast access waveguides [5]. However, in some technologies these approaches may not work. There may not be room for dummy waveguides, or reduced contrast may not be offered by the technology platform. In [6], the corners of the MMI were cut to reduce reflections. Here we take the MMI structure of [6] as a starting point, and add additional structures to reduce reflections. The approach we present can be used in any technology that offers designers to freely determine the waveguide shape in the plane.

II. Design

We consider deep-etched ridge waveguides in an indium phosphide based generic integration technology, with the layer stack shown in Fig. 1. The described approach can be applied equally well to other technologies such as silicon on insulator. The waveguides are defined by surrounding them with deep-etched trenches of width w_t. As a result, most of the chip surface remains unetched. This stabilizes dry-etch rates, improves mechanical robustness, and eases planarization.

Fig. 2 shows the proposed layout of the etched areas that together define the MMI combiner. The parameters L_MMI, W_MMI, w_a and o, are the regular MMI parameters for the length, width, access waveguide width, and offset, respectively. The offset is defined with respect to the MMI center line. In addition, the angles α_1 through α_4, together with width w_1 and trench width w_t, define the shape of the etched regions. All surfaces where reflection could occur are angled in this layout. Additionally, the openings on the top and bottom of the MMI allow light to continue propagating to a slab region, instead of

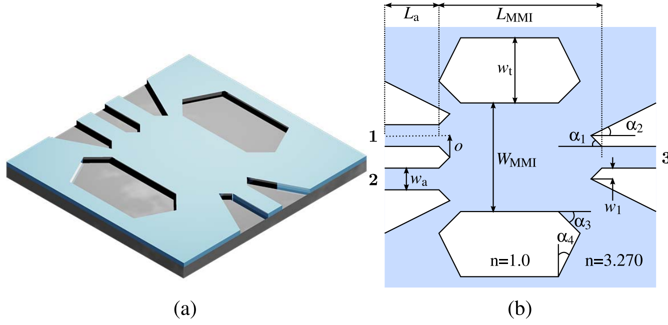

Fig. 2. Low reflection MMI combiner layout. (a) 3D view of the device layout. (b) 2D top view. The lighter areas are deeply-etched. The port numbers are indicated by the bold numbers.

TABLE I
FABRICATED MMI PROPERTIES

Design ID	Type	L µm	W µm	w_a µm	o µm	α_1 [°]	α_2 [°]	α_3 [°]	α_4 [°]
A	Regular	26.4	5.0	1.5	±1.2	-	-	-	-
B	Cut	26.4	5.0	1.5	±1.2	60	-	-	-
C	Cut	26.4	5.0	1.5	±1.2	30	-	-	-
D	LR	26.4	5.0	1.5	±1.2	60	20	60	15
E	LR	26.4	5.0	1.5	±1.2	60	10	60	15
F	LR	26.4	5.0	1.5	±1.2	30	20	60	15
G	LR	26.4	5.0	1.5	±1.2	30	10	60	15

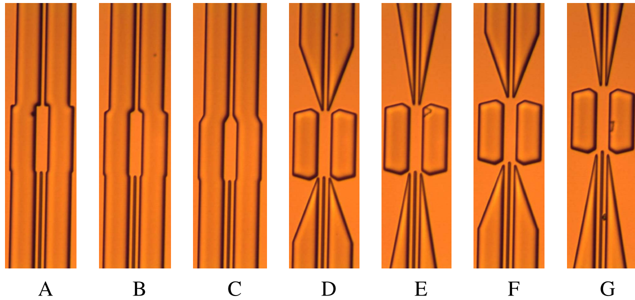

Fig. 3. Optical microscope image of the fabricated devices. Devices D through G use the new layout.

scattering backward. Care should be taken that this light does not couple into other structures further along the slab. This could be avoided by placing absorbing material some distance away from the MMI.

We will compare the performance of the new proposed layout to two previously reported MMI layouts. These are the the regular rectangular layout, and the shape described in [6]. We refer to the first shape as 'Regular', and to the second as 'Cut'. A number of devices of these two types were also included in our study to serve as reference devices. A total of seven devices were designed for the layer stack of Fig. 1, which has an effective slab index of 3.27 at a wavelength of 1550 nm. Their parameters are shown in Table I, and an image of each fabricated device is in Fig. 3. The basic parameters like L_{MMI}, W_{MMI}, w_{a} and o are the same for all devices. We varied the values for the angles α_1 and α_2. The angle α_3 was kept fixed at 60° and α_4 was fixed at 15°. The width w_1 is determined by the minimum lithographical feature size. This width was fixed at 0.4 μm. The trench width w_{t} was set to 10μm.

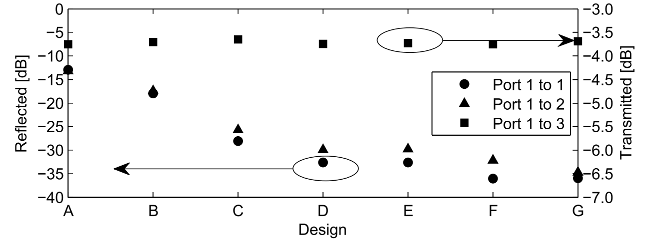

Fig. 4. FDTD simulation result. Reflection level from port 1 to port 1 and from port 1 to port 2 is shown on the left y-axis. The transmitted light from port 1 to port 3 is shown on the right y-axis. A low reflection of around −35 dB can be obtained by setting $\alpha_1 = 30°$ and $\alpha_2 = 10°$.

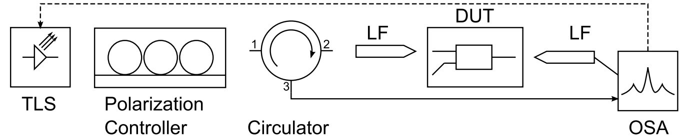

Fig. 5. Measurement setup. TLS: tunable laser source, LF: lensed fiber, DUT: device under test, OSA: optical spectrum analyzer. The optical spectrum analyzer is synchronized to the TLS. This strongly suppresses ASE noise from the laser and enables high dynamic range.

III. SIMULATION

The amount of reflection in each of the designs was numerically evaluated using a commercially available 2D Finite Difference Time Domain method [7]. An effective slab index of 3.27 was used for the non-etched areas, and index 1.0 for the etched areas where semi-conductor material was replaced by air. An 80 fs long modal pulse centered at a wavelength of 1550 nm was used as the starting field for the simulation. The pulse was launched into port 1. The total simulated time was around 1 ns in order to obtain 110 unique samples in the wavelength range from 1500 nm to 1600 nm. In order to easily compare the performance of the different devices, we took the average value over the recorded spectra.

Fig. 4 shows the simulation results for the various devices. The parasitic reflections from port 1 to port 1 and from port 1 to port 2 are suppressed, as indicated by the triangular and circular shapes in Fig. 4. The 'Regular' MMI, labeled A, has reflection levels of around −13 dB. The 'Cut' MMI proposed earlier can reduce this to −26 dB. The simulation indicates that our device design can reach reflection levels of −35 dB. Fig. 4 also shows the transmission from port 1 to 3 and that it is not affected by the change in shape of the MMI.

IV. MEASUREMENT

The devices were fabricated at NanoLab@TU/e, in an all-deep indium phosphide generic integration technology. The devices were characterized by making a wavelength sweep. The measurement setup used is shown in Fig. 5. An Ando AQ4320A tunable laser is controlled by an optical spectrum analyzer (Ando AQ6317) and the transmitted and reflected power is recorded as a function of wavelength. A laser power of 5 dBm was used and the OSA bandwidth was set to 2 nm. The chip was temperature stabilized at 25 °C by a Peltier element. We refer to the signal going from the first lensed fiber to the second lensed fiber as 'forward', and to the signal at port 3 of the circulator as 'backward'. A polarization controller was used to ensure that only TE polarized light was coupled into

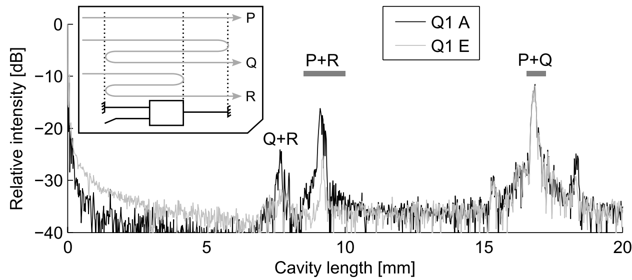

Fig. 6. Example length domain signals for devices A and E from quarter Q1. The inset shows the possible paths (P,Q,R) through the chip. The bars above the peaks show the integration range used. Path Q+R is not used.

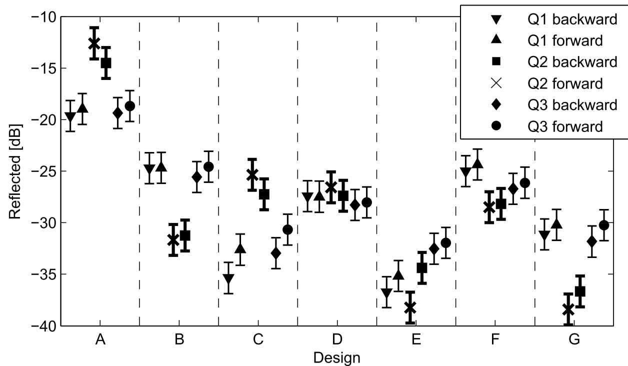

Fig. 7. Measurement results of reflection level from MMI port 1 to port 1. The forward points are obtained by analyzing the transmitted signal, the backward points by analyzing the reflected signal. Q1, Q2, and Q3 indicate three separately processed quarters of an InP wafer. Q1 and Q3 have an etch depth of 3.16 μm. Q2 was intentionally etched deeper, down to 3.33 μm.

the chip. Port 1 and port 3 of the MMI are led to straight facets using mono-mode waveguides. MMI port 2 is led to an angled facet, which strongly suppresses reflections from that point.

The parasitic reflections of the different devices are evaluated as follows. First a wavelength sweep from 1520 nm to 1580 nm with 12001 points was performed. Each uncoated straight facet gives a reflection of around 30 %. There are now multiple possible paths light can take through the chip. Light from each path can interfere with light from each other path. By taking a Fourier transform of the wavelength spectrum, a length domain signal is obtained, where each combination of paths causes a peak to appear at the length difference between paths. The peak height is determined by the relative total path loss in both paths. Fig. 6 shows the Fourier transformed signal, and the identified paths (P,Q,R) together with their associated peaks. By integrating over a peak, its energy content can be determined. Each peak can be normalized with respect to the peak formed by paths P and Q. For proper normalization, the waveguide propagation loss needs to be known. This was determined to be 2.0 dB/cm in a separate measurement. The magnitude of the parasitic MMI reflection follows from the peak height of paths P and R. This method can be applied to either the forward or backward signal. Only the response from MMI port 1 back to port 1 was characterized. The simulations of the previous section show that the reflection level from port 1 to port 2 is very similar.

The results of the analysis of the measurement data is shown in Fig. 7. An uncertainty margin of ± 1.5 dB is indicated. Around 1 dB comes from uncertainties in the MMI transmission, 0.3 dB from uncertainties in facet reflection, and 0.2 dB from waveguide losses. Devices from three quarters (Q1, Q2, Q3) of the same wafer that were processed separately, were characterized. Q1 and Q3 were etched 650 nm below the core, while Q2 was intentionally etched deeper to 880 nm below the core. Fig. 7 clearly shows that quarters Q1 and Q3 behave similarly. For some devices from Q2 the measured value deviates from Q1 and Q3. The LR devices from Q2 perform either the same or better, which indicates that they are more tolerant to variations in etch-depth. In all cases, the values obtained for the forwards and backward measurements are very similar. For Q1 and Q3, the regular and cut devices perform better than expected from simulation. This can be explained by the fact that the waveguide sidewalls are not perfectly vertical, which is assumed in the simulation. The simulation showed only a small difference in reflection level between $\alpha_2 = 20°$ and $\alpha_2 = 10°$. The measurements indicate a stronger dependence on this angle, with $\alpha_2 = 10°$ performing significantly better. The measured values for the design with $\alpha_1 = 30°$ also differ notably from the simulated values. This is quite surprising, because when looking at Fig. 2(b), it is clear that the influence of α_1 on the geometry is much less than that of α_2. A possible explanation for the observed difference with simulation results is a change in fabrication tolerance from device to device. A simulation, in which all widths were increased by 0.1μm showed a slightly lower tolerance for the new design (3 dB higher reflection vs 1 dB), but no dependency on α_1. Taking the average over all measurements, device E performs the best with -34.8 dB. The best of the Cut MMIs is C with -27.5 dB on average. This is a 7.3 dB improvement, and a 17.5 dB improvement when compared to the regular MMI.

V. Conclusion

It was shown experimentally that the reflection level in deep-etched, high-contrast MMIs can be reduced to -34.8 dB by optimizing the MMI geometry. This means a strong reduction in parasitic reflections can be accomplished with respect to the standard MMI. The improvement with respect to MMIs with angled back-walls is 7.3 dB. This approach can be applied to technologies that use trenches to define waveguides.

References

[1] D. Erasme, L. H. Spiekman, C. G. P. Herben, M. K. Smit, and F. H. Groen, “Experimental assessment of the reflection of passive multimode interference couplers,” *IEEE Photon. Technol. Lett.*, vol. 9, no. 12, pp. 1604–1606, Dec. 1997.

[2] Y. Gottesman, E. V. K. Rao, and B. Dagens, “A novel design proposal to minimize reflections in deep-ridge multimode interference couplers,” *IEEE Photon. Technol. Lett.*, vol. 12, no. 12, pp. 1662–1664, Dec. 2000.

[3] E. Pennings, R. van Roijen, M. J. N. van Stralen, P. J. de Waard, R. G. M. P. Koumans, and B. H. Verbeck, “Reflection properties of multimode interference devices,” *IEEE Photon. Technol. Lett.*, vol. 6, no. 6, pp. 715–718, Jun. 1994.

[4] L. Soldano and E. Pennings, “Optical multi-mode interference devices based on self-imaging: Principles and applications,” *J. Lightw. Technol.*, vol. 13, no. 4, pp. 615–627, Apr. 1995.

[5] Y. Li and R. Baets, “Improved multi-mode interferometers (MMIs) on silicon-on-insulator with the optimized return loss and isolation,” in *Proc. 16th Ann. Symp. IEEE Photonon. Benelux Chapter*, Jan. 2011, pp. 1–4.

[6] R. Hanfoug, *et al.*, “Reduced reflections from multimode interference couplers,” *Electron. Lett.*, vol. 42, no. 8, pp. 465–466, Apr. 2006.

[7] PhoeniX Software B.V., Enschede, The Netherlands. (2013). *OptoDesigner V4.3.2* [Online]. Available: http://www.phoenixbv.com